NATIONAL ADVISORY COMMITTEE FOR AERONAUTICS

WARTIME REPORT

ORIGINALLY ISSUED
February 1944 as
Advance Confidential Report 4B04

COMPARISON OF CALCULATED AND EXPERIMENTAL PROPELLER CHARACTERISTICS FOR FOUR-, SIX-, AND EIGHT-BLADE SINGLE-ROTATING PROPELLERS

By John L. Crigler

Langley Memorial Aeronautical Laboratory
Langley Field, Va.

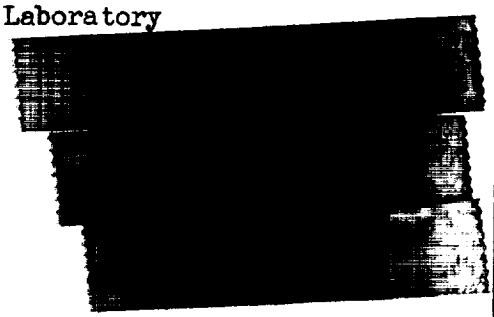

NACA

NATIONAL ADVISORY COMMITTEE FOR AERONAUTICS

ADVANCE CONFIDENTIAL REPORT

COMPARISON OF CALCULATED AND EXPERIMENTAL PROPELLER CHARACTERISTICS FOR FOUR-, SIX-, AND EIGHT-BLADE SINGLE-ROTATING PROPELLERS

By John L. Crigler

SUMMARY

The calculated performance of four-, six-, and eight-blade single-rotating propellers has been compared with experimental results for blade angles ranging from 25° to 65°. The experimental data were obtained on propellers mounted in front of a streamline body with a spinner housing the hub. The calculated propeller performance was found to be in good agreement with the experimental results over the complete range of blade angle investigated. The method of calculations is presented in detail and a sample computation is included.

INTRODUCTION

The selection of a propeller for a new airplane design may be based on either wind-tunnel test data or theoretical calculations. If test data are used, empirical corrections are applied, if required, for changes in number of blades, activity factor, blade thickness, airfoil section, Mach number, and body shape. If these empirical corrections are large, they become the determining factor in selecting the propeller for the design application. The selection of propellers based on theoretical calculations has been open to considerable question because the theory strictly applies only to the idealized propeller. From time to time calculated results have been compared with experimental data for a few blade angles, but a comparison over a wide range of blade angle for a propeller operating at conditions giving nonoptimum load distribution has been lacking.

A method of analysis is presented in detail and calculated results are compared with experimental results on single-rotating propellers of four, six, and eight blades for blade-angle settings of 25°, 35°, 45°, 55°, and 65° at the 0.75 radius. The propeller tests (references 1 and 2) of the Hamilton Standard propeller 3155-6 afford an excellent opportunity for making such a comparison. On this test setup the interference drag was small, the velocity distribution in the plane of the propeller was approximately free stream, and the airfoil section characteristics were available for the test Mach numbers. This information permitted a direct check between propeller theory and experimental results without the use of empirical corrections.

The method of calculations is based on the propeller theory as used by Lock. The correction factors for a finite number of blades as obtained from Goldstein (for the two-blade propeller and extended by Lock for other blade numbers) are strictly limited to a very light loading and to a particular distribution of circulation along the blade. For this reason there has been some hesitancy in using the Goldstein corrections for any other distributions of loading. The optimum distribution of loading is herein compared with the actual distribution for the Hamilton Standard propeller 3155-6 at a number of operating conditions. The degree to which the calculated and experimental propeller characteristics agree over the entire range of blade angle is an indication of the validity of the correction factors.

SYMBOLS

a	axial-velocity interference factor
B	number of propeller blades
b	chord of propeller blade element
C_D	section drag coefficient $\left(D_o/\frac{1}{2}\rho V^2 b\right)$
C_L	section lift coefficient $\left(L/\frac{1}{2}\rho V^2 b\right)$
C_P	power coefficient $\left(P/\rho n^3 D^5\right)$

C_Q	torque coefficient $\left(Q/\rho n^2 D^5\right)$
C_T	thrust coefficient $\left(T/\rho n^2 D^4\right)$
D	propeller diameter
D_o	drag of blade element
F	Goldstein correction factor for finite number of blades
h	thickness of propeller blade element
J	advance-diameter ratio (V/nD)
L	lift of blade section
n	rotational speed of propeller, revolutions per second
p	geometric pitch of propeller
P	input power of propeller
Q	torque of propeller
r	radius to any blade element
R	tip radius
T	thrust of propeller
V	axial velocity of propeller
x	radial location of blade element (r/R)
α	angle of attack
β	propeller blade angle at 0.75 radius
γ	$\tan^{-1} \frac{C_D}{C_L}$
ϵ	angle of inflow $(\phi - \ell_o)$
θ	propeller blade angle at radius r
ρ	mass density of air

σ propeller element solidity $(Bb/2\pi r)$

ϕ_o angle of advance of propeller $\left(\tan^{-1}\frac{V}{\pi nDx}\right)$

ϕ angle of resultant velocity to plane of rotation

η propeller or element efficiency

BASIC DATA AND METHODS

The characteristics for the airfoil sections from $x = 0.45$ to $x = 0.95$ given in figures 1 and 2 were taken from reference 3. The section at the 0.45 radius is a modified Clark Y section and the sections from the 0.6 radius to the tip are Clark Y sections. Data for the section thicknesses used were obtained by cross fairing. The section at $x = 0.3$ was arbitrarily given a C_D of 0.10 and a slope of lift curve of 0.045 per degree with zero lift at $\alpha = 0^\circ$. The characteristics at $x = 0.3$ are only approximate but, since the torque absorbed at this radius is small, the use of these characteristics is considered satisfactory. Inasmuch as the average spinner radius for the experimental results of references 1 and 2 was 0.21R, the calculated curves presented herein were cut off at the 0.21 radius, although the section at the 0.2 radius was computed to aid in fairing the curves. The section at the 0.2 radius is almost circular and was assumed to operate at zero lift and constant C_D of 0.4.

The method used for computing the element thrust and element torque coefficients is given in detail with a sample computation. The following data are required:

(1) The propeller blade plan form and pitch distribution (fig. 3)

(2) The number of blades

(3) The lift and drag characteristics of the blade sections at each radius (figs. 1 and 2)

Element calculations can be made for as many radii as desired. In making these element calculations the blade angle at each radius and the operating V/nD are required. The procedure at radius x follows:

(1) Obtain ϕ_o from

$$\phi_o = \tan^{-1} \frac{V/nD}{\pi x}$$

(2) Obtain $\alpha + \epsilon$ from

$$(\alpha + \epsilon) = (\theta - \phi_o)$$

where θ is the blade angle at the chosen radius.

(3) Assume a value of α and obtain the corresponding value of C_L from airfoil section characteristics.

(4) Find ϵ from the formula

$$\tan \epsilon = \frac{\sigma C_L}{4F \sin \phi}$$

Using ϕ_o, instead of ϕ, and F obtained from ϕ_o gives an approximation to ϵ. Using ϕ equal to $\phi_o + \epsilon_{approx}$ gives a second approximation to ϵ. The value of ϵ is thus found by successive approximations, but the second approximation usually gives ϵ to the desired degree of accuracy. (Fig. 4, taken from reference 4, may be used in finding ϵ instead of solving the equation $\tan \epsilon = \frac{\sigma C_L}{4F \sin \phi}$. In this figure, ϵ is given in terms of nDx/V and $\sigma C_L/F$ instead of as a function of ϕ. In this case, the first approximation is usually sufficiently accurate, the only approximation being the use of F based on ϕ_o instead of ϕ.)

(5) Determine F from figure 5 (data taken from reference 5), where F is plotted against ϕ.

(6) Repeat calculations of α and ϵ with the new assumed α from step (3) and plot α against $\alpha + \epsilon$. This plot aids in reducing calculations because the value of $\alpha + \epsilon$ that equals $\theta - \phi_o$ gives the desired α and ϵ.

(7) Find γ from

$$\tan \gamma = \frac{C_D}{C_L}$$

The final torque and thrust coefficients are thus given as

$$\frac{dC_Q}{dx} = \frac{F}{2} \pi^3 x^4 \frac{\epsilon}{57.3} \frac{1 + \cot \phi \tan \gamma}{\left(\cot \phi + \frac{\epsilon}{57.3}\right)^2}$$

$$\frac{dC_T}{dx} = F\pi^3 x^3 \frac{\epsilon}{57.3} \frac{\cot \phi - \tan \gamma}{\left(\cot \phi + \frac{\epsilon}{57.3}\right)^2}$$

The contributions of thrust and torque at the 0.2 radius were computed on the assumption that there was no lift on this section. The value of C_L was accordingly put equal to zero and the axial inflow was neglected in the calculations. The element thrust coefficient

$$\frac{dC_T}{dx} = \frac{BbJ^2}{8R} \frac{(1 + a)^2}{\sin^2 \phi} (C_L \cos \phi - C_D \sin \phi)$$

reduces to

$$\frac{dC_T}{dx} = -\sigma C_D \frac{\pi x}{4} J\sqrt{J^2 + (\pi x)^2}$$

$$= -\sigma C_D \frac{\pi x}{4} \frac{J^2}{\sin \phi}$$

and the element torque coefficient

$$\frac{dC_Q}{dx} = \frac{BbJ^2 x}{16R} \frac{(1 + a)^2}{\sin^2 \phi} (C_L \sin \phi + C_D \cos \phi)$$

reduces to

$$\frac{dC_Q}{dx} = \sigma C_D \frac{\pi^2 x^3}{\varepsilon} \sqrt{J^2 + (\pi x)^2}$$

$$= \sigma C_D \frac{\pi^2 x^3}{8} \frac{J}{\sin \phi}$$

As an example in the use of the method, computations are given in table I for the four-blade single-rotating propeller having a Hamilton Standard 3155-6 blade set at 45° at the 0.75 radius and operating at a V/nD of 1.8. The differential-thrust and the differential-torque distribution from table I is plotted in figure 6. Curves of this type were constructed and from them the calculated propeller characteristics were made. (See figs. 8 to 13.) The range of the calculated curves is limited to the stalling angles of the airfoil sections, the maximum allowable value of the lift coefficient at any section being about 1.0. This value depends on the airfoil section and its thickness ratio.

RESULTS AND DISCUSSION

The factor F, which is a correction for finite number of blades as given by Goldstein's analysis, is derived for the case of a very light loading and a particular distribution of circulation along the blade. The suitability of this factor for computing the performance of propellers with other loadings is determined by comparison with experimental results. The calculated distributions of the element load coefficient for the test propeller at several operating conditions are compared in figure 7 with the optimum distributions from reference 4. Although the distribution varies widely from the optimum in many cases, notably at high values of V/nD, the computed propeller coefficients are in close agreement with the experimental values. It is therefore concluded that the correction factors are sufficiently accurate for practical propeller calculations.

The experimental propeller characteristics of the single-rotating four- and six-blade propellers (reference 1) and of the eight-blade propeller (reference 2) are compared with the calculated characteristics in figures 8 to 13. Figure 14 is a composite of the thrust curves for easy comparison. The agreement is very good in all cases except for the eight-blade propeller when $\beta = 55^\circ$ and 65°.

Figure 15 compares the experimental and calculated efficiencies of the four-, six-, and eight-blade propellers over the entire range of blade angle. As would be expected, the calculated values give smoothly faired curves, which show that the highest efficiency envelope is obtained with the four-blade propeller and the lowest efficiency with the eight-blade propeller. The experimental curves show the same trends and the variations between the two sets are considered to be within the accuracy of the tests, the main discrepancy being at the 65° blade-angle settings.

CONCLUSION

The calculated and experimental performances of four-, six-, and eight-blade single-rotating propellers have been compared. It is concluded from this comparison that the performance of a propeller can be accurately calculated if the velocity distribution in the plane of the propeller, the propeller airfoil section characteristics, and the propeller plan form are known.

Langley Memorial Aeronautical Laboratory,
National Advisory Committee for Aeronautics,
Langley Field, Va.

REFERENCES

1. Biermann, David, and Hartman, Edwin P.: Wind-Tunnel Tests of Four- and Six-Blade Single- and Dual-Rotating Tractor Propellers. Rep. No. 747, NACA, 1942.

2. Biermann, David, and Gray, W. H.: Wind-Tunnel Tests of Eight-Blade Single- and Dual-Rotating Propellers in the Tractor Position. NACA A.R.R., Nov. 1941.

3. Pinkerton, Robert M., and Greenberg, Harry: Aerodynamic Characteristics of a Large Number of Airfoils Tested in the Variable-Density Wind Tunnel. Rep. No. 628, NACA, 1938.

4. Crigler, John L., and Talkin, Herbert W.: Propeller Selection from Aerodynamic Considerations. NACA A.C.R., July 1942.

5. Lock, C. N. H., and Yeatman, D.: Tables for Use in an Improved Method of Airscrew Strip Theory Calculation. R. & M. No. 1674, British A.R.C., 1935.

TABLE I.- COMPUTATION OF PROPELLER THRUST AND TORQUE COEFFICIENTS

$[\beta = 45^\circ;\ V/nD = 1.8;\ B = 4]$

x	$\frac{V/nD}{\pi x}$	ϕ_o	θ	$\alpha+\epsilon$	σ	α	ϵ	ϕ	F	C_L	L/D	$\tan\gamma$	$\cot\phi$	dC_Q/dx	dC_T/dx
0.3	1.9099	62.36	66.85	4.49	0.212	3.95	0.54	62.90	1.091	0.177	1.77	0.5650	0.5117	0.0061	-0.0017
.45	1.2732	51.85	57.50	5.65	.1935	2.85	2.80	54.65	.917	.758	59.7	.0168	.7094	.0502	.1524
.6	.9549	43.68	50.45	6.77	.1681	3.60	3.17	46.85	.788	.762	77.0	.0130	.9374	.0900	.2737
.7	.8185	39.30	46.65	7.35	.1380	4.23	3.12	42.42	.698	.748	76.4	.0131	1.0944	.1088	.3355
.8	.7162	35.61	43.45	7.84	.1041	4.72	3.12	38.73	.586	.773	75.1	.0133	1.2469	.1217	.3693
.9	.6366	32.48	40.85	8.37	.0717	5.08	3.29	35.77	.422	.792	73.1	.0137	1.3381	.1201	.3601
.95	.6031	31.09	39.70	8.61	.0541	5.06	3.55	34.64	.301	.783	72.1	.0139	1.4474	.1058	.3120

x	σ	σC_D	$\frac{\pi x}{4}$	$(\pi x)^2$	$\frac{J}{\sin\phi}$	$\frac{\pi^2 x^3}{8}$	dC_Q/dx	dC_T/dx
0.2	0.255	0.102	0.1571	0.395	1.907	0.0099	0.0019	-0.0550

L-362

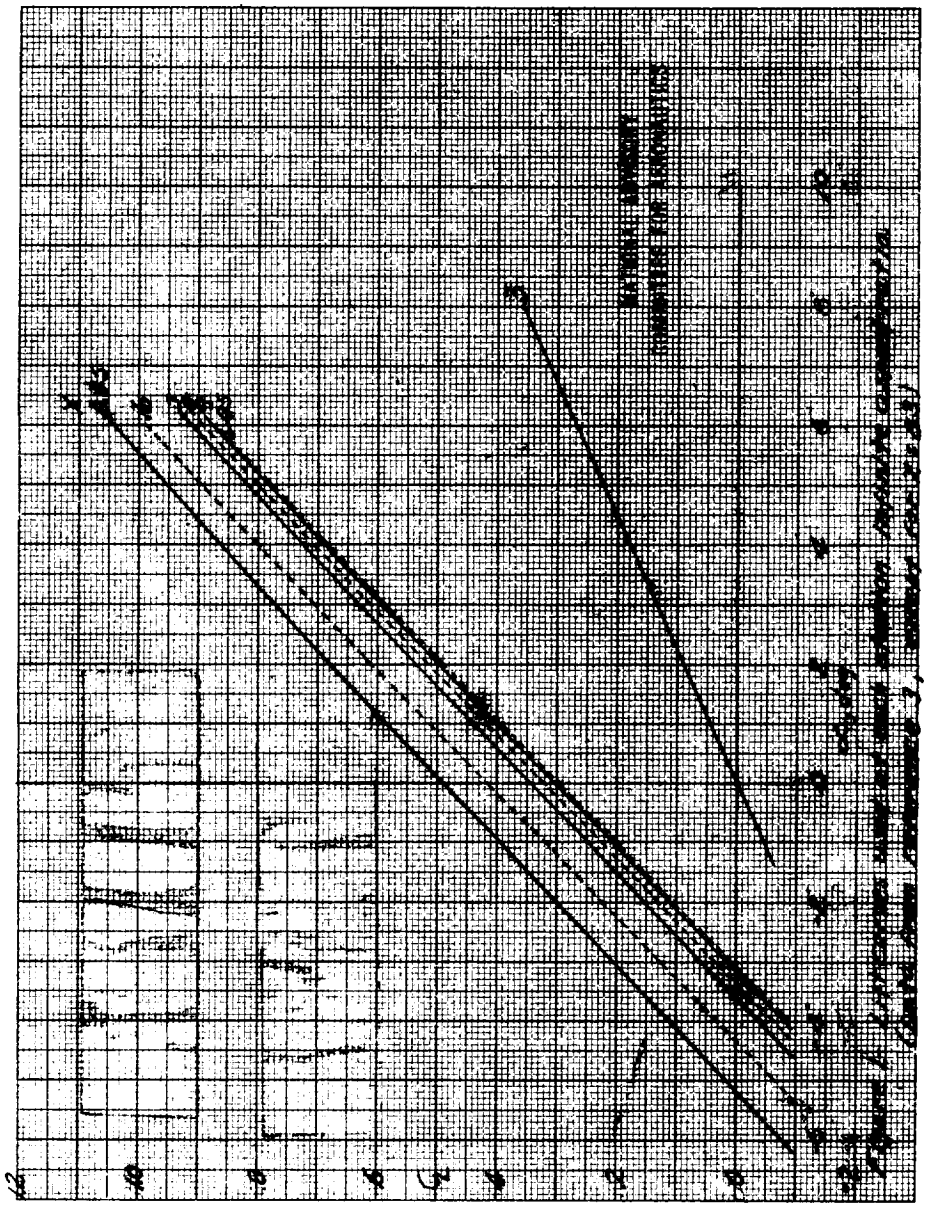

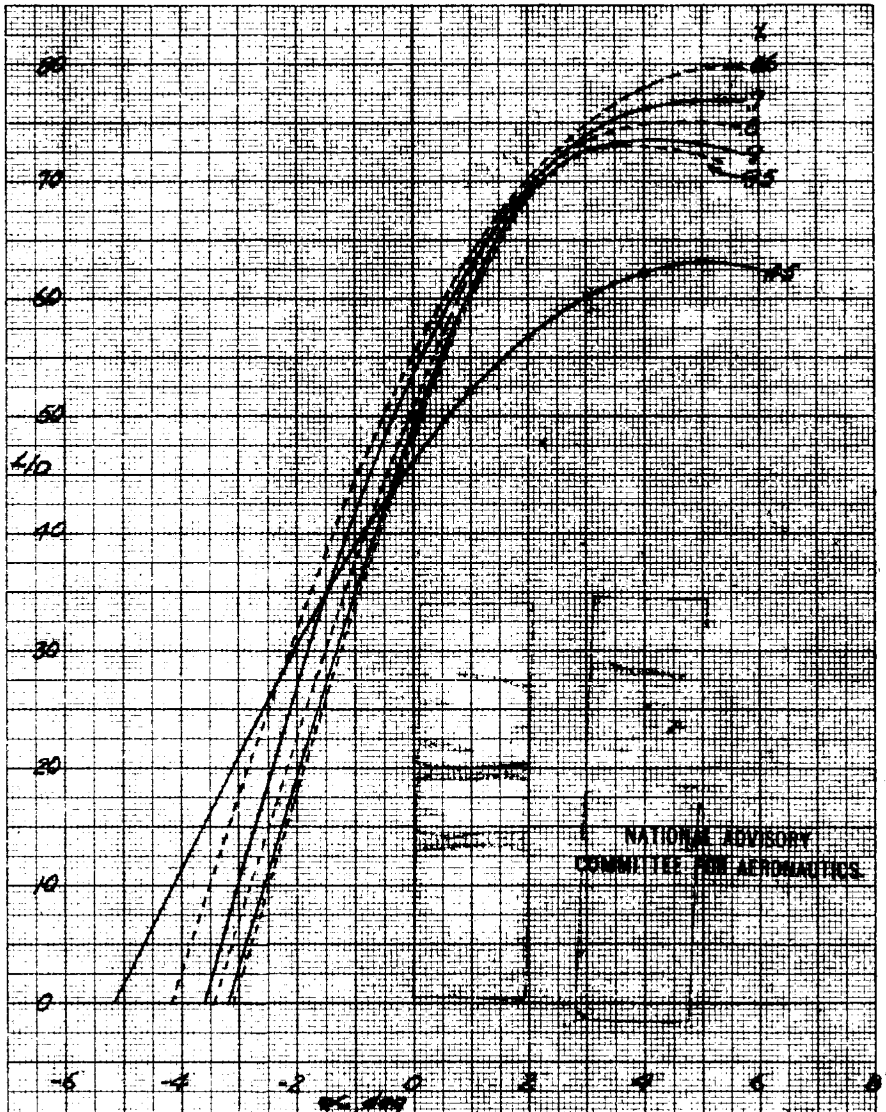

Figure 2.- Lift-drag curves used at each station. Infinite aspect ratio (data from reference 3).

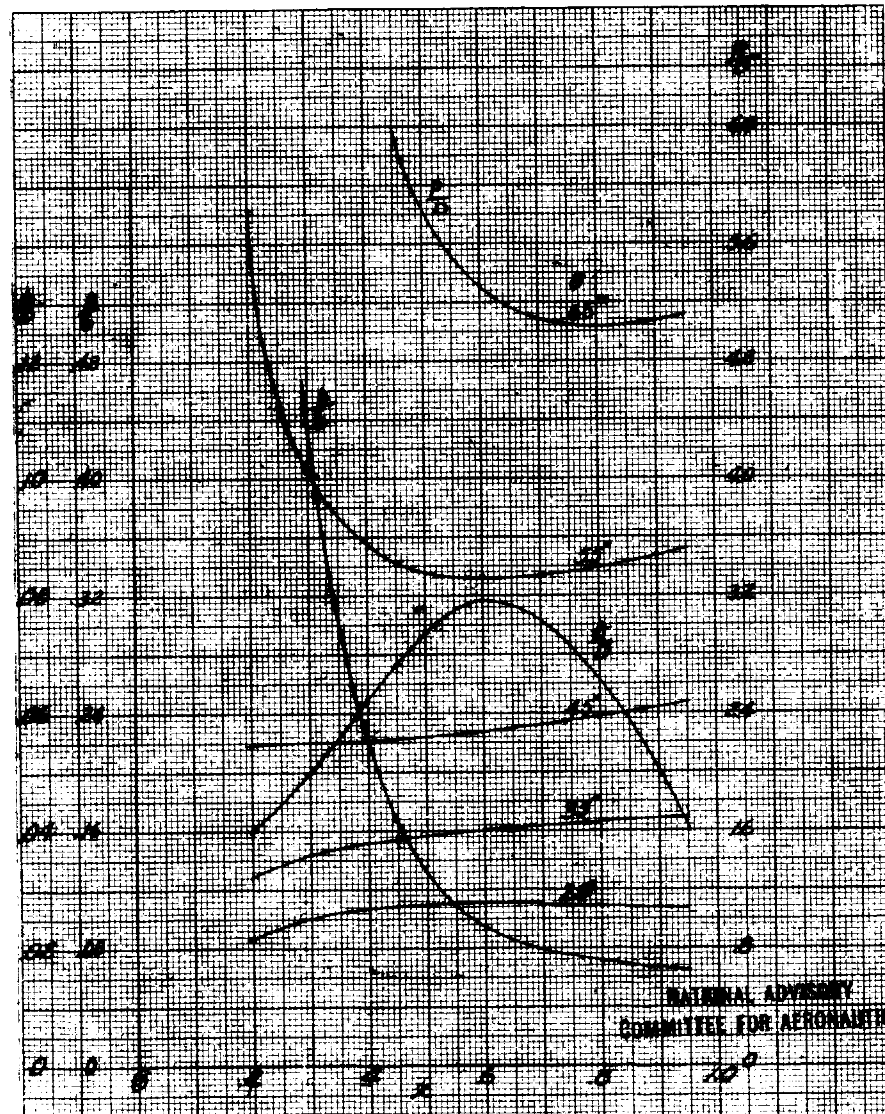

Figure 3.- Blade form curves for propeller 8125-6.

L-362

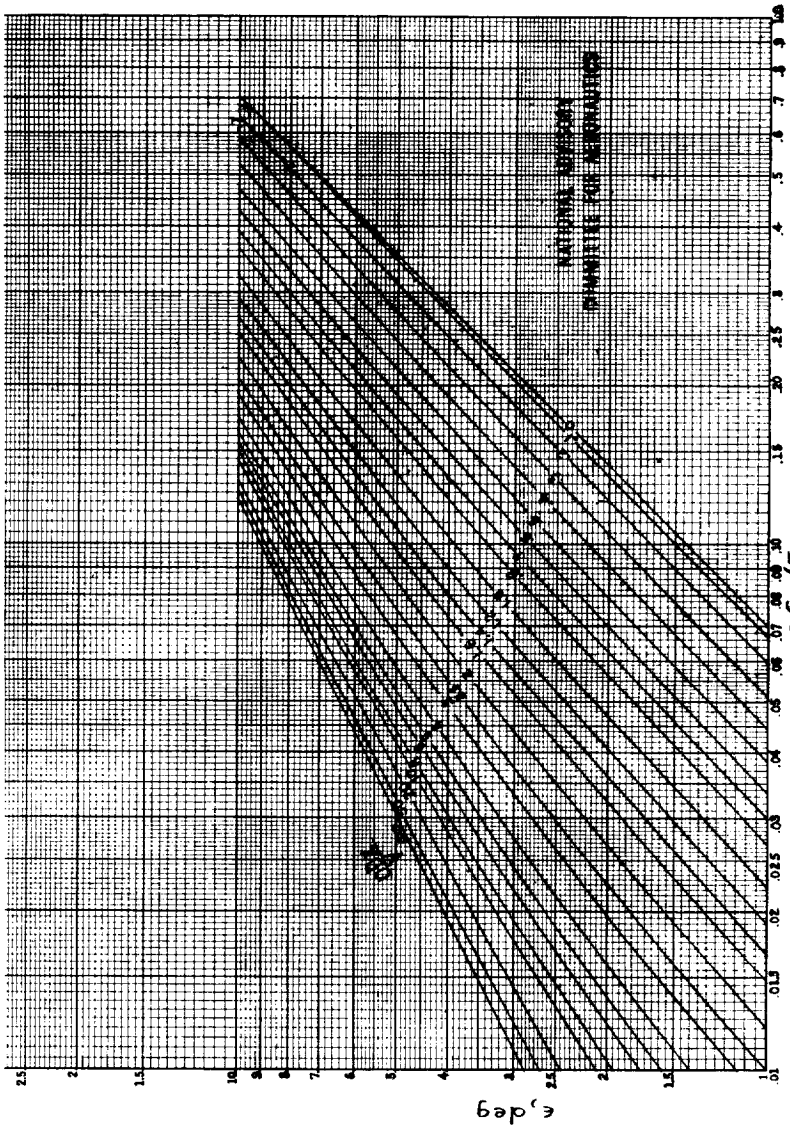

Figure 4. – Chart of ϵ against $\frac{\sigma C_L}{F}$ for values of $\frac{D_1 x}{V}$ from 0 to ∞. (from reference 4.)

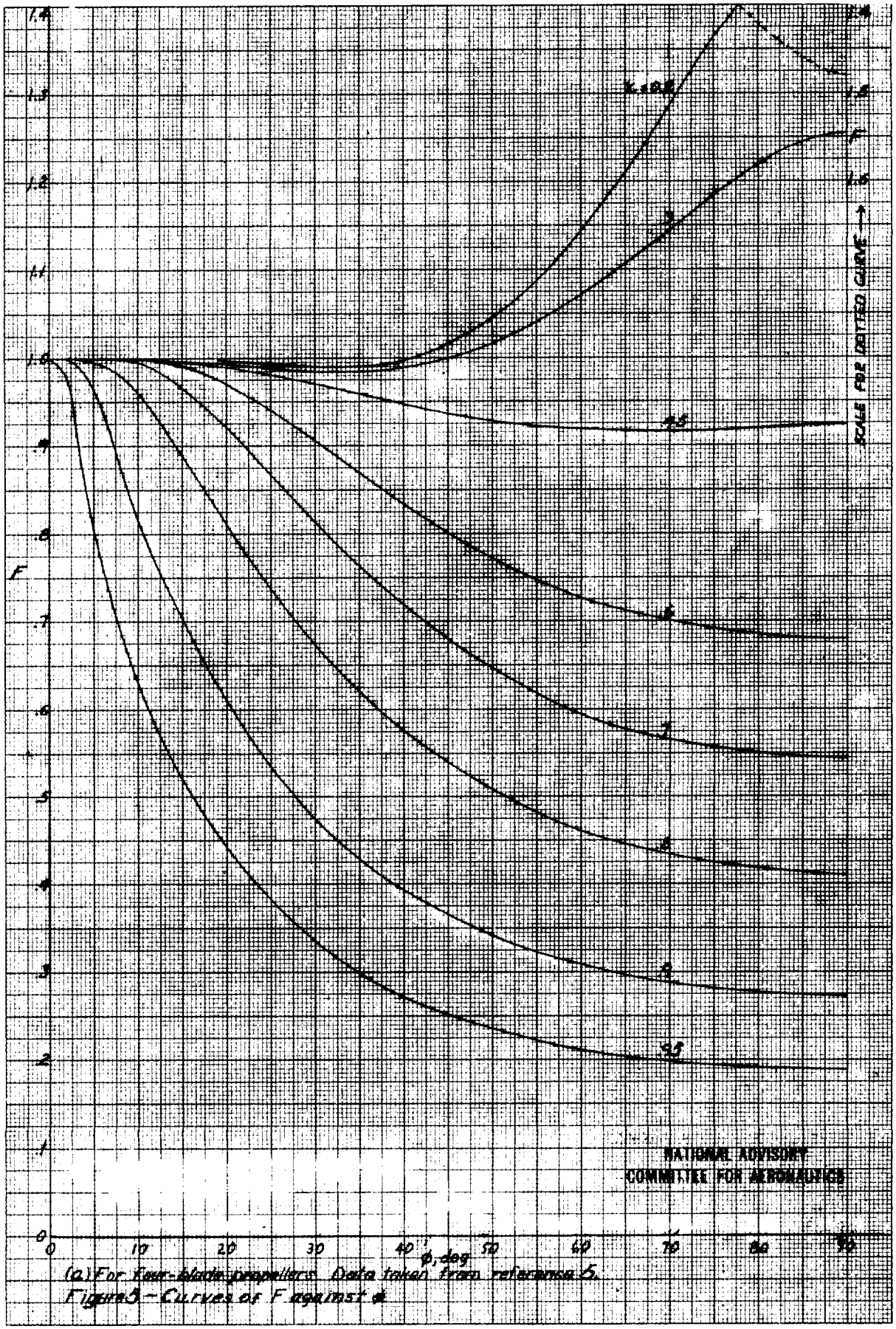

(a) For four-blade propellers. Data taken from reference 5.

Figure 5 - Curves of F against φ

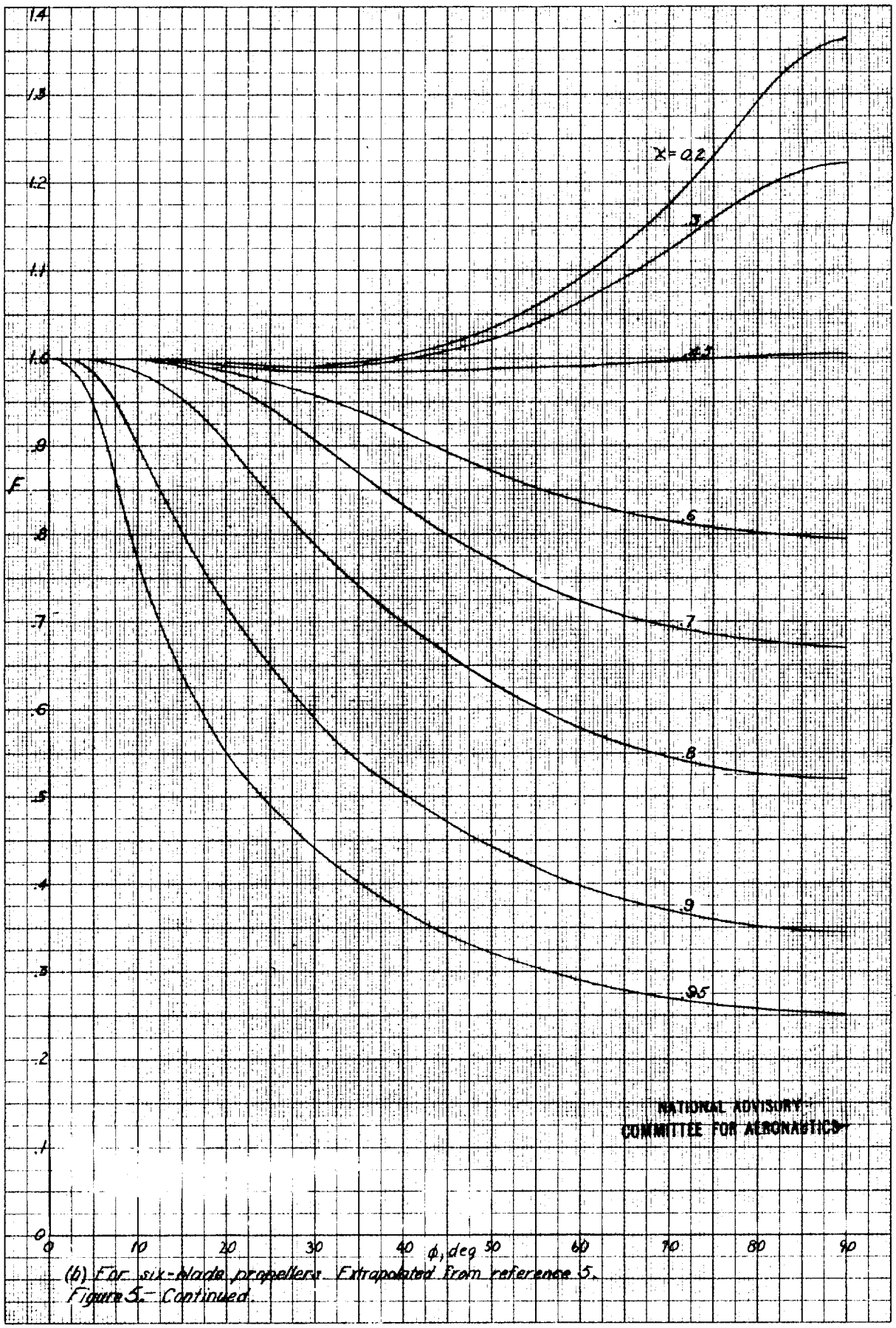

(b) For six-blade propellers. Extrapolated from reference 5.

Figure 5.- Continued.

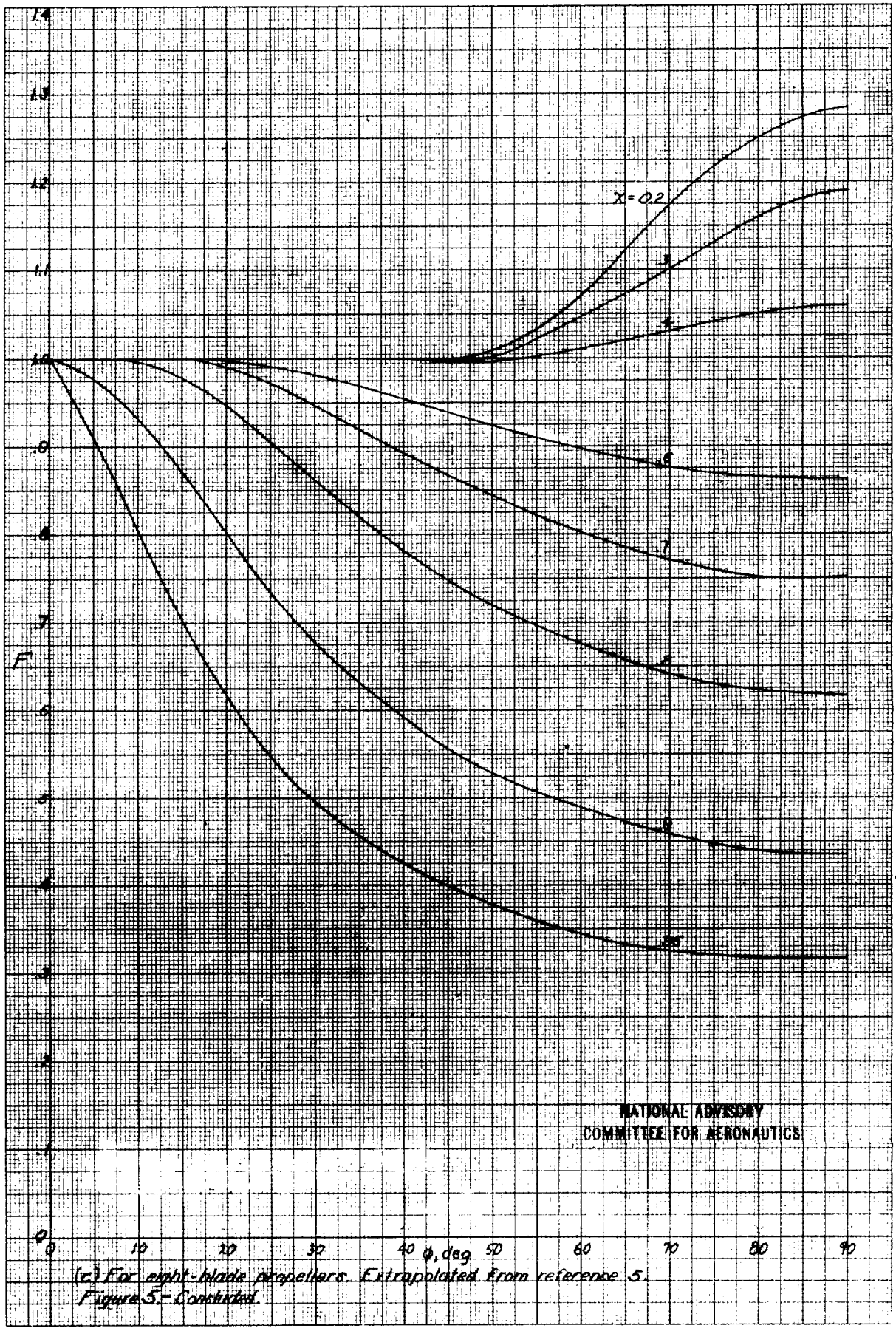

(c) For eight-blade propellers. Extrapolated from reference 5.

Figure 5.- Concluded.

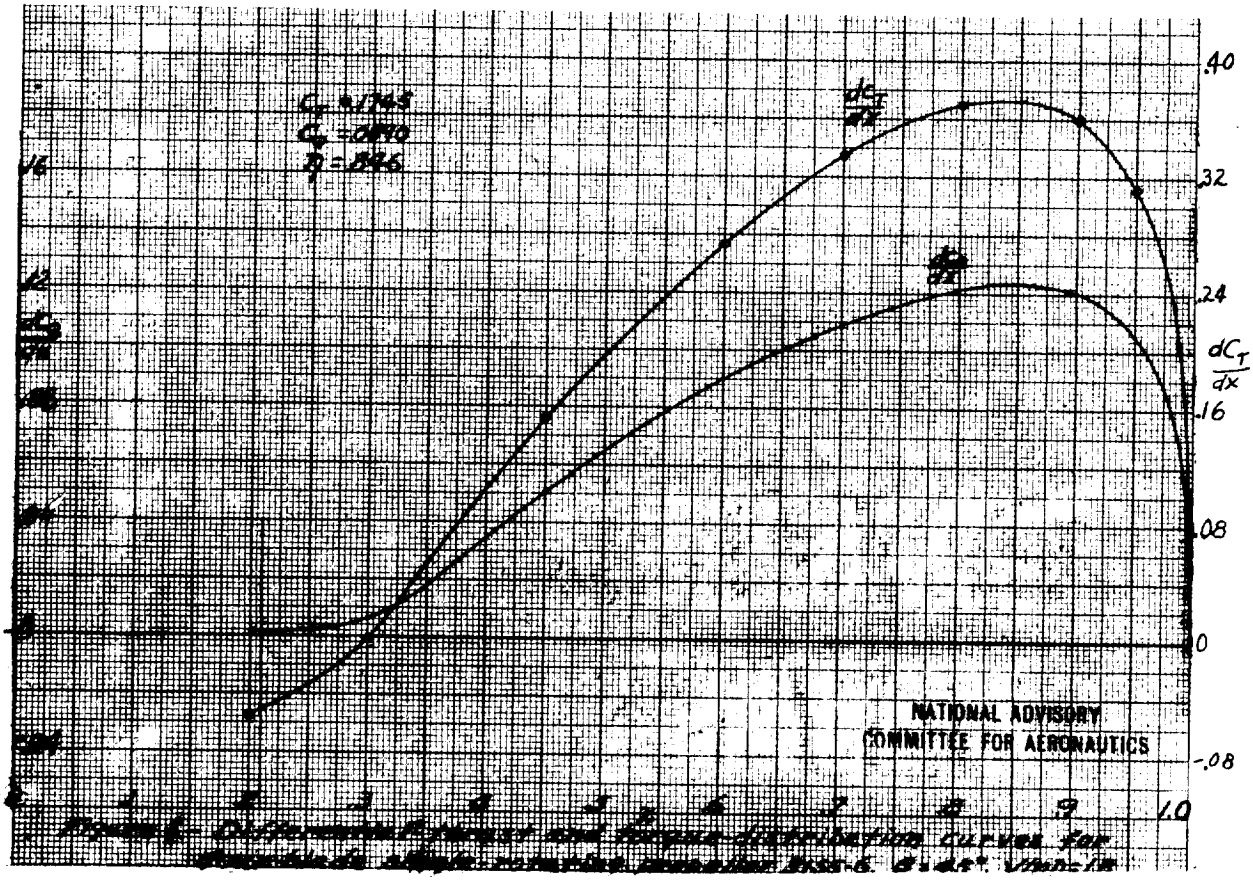

Figure 6 - Differential-thrust and torque-distribution curves for propeller 3155-6.

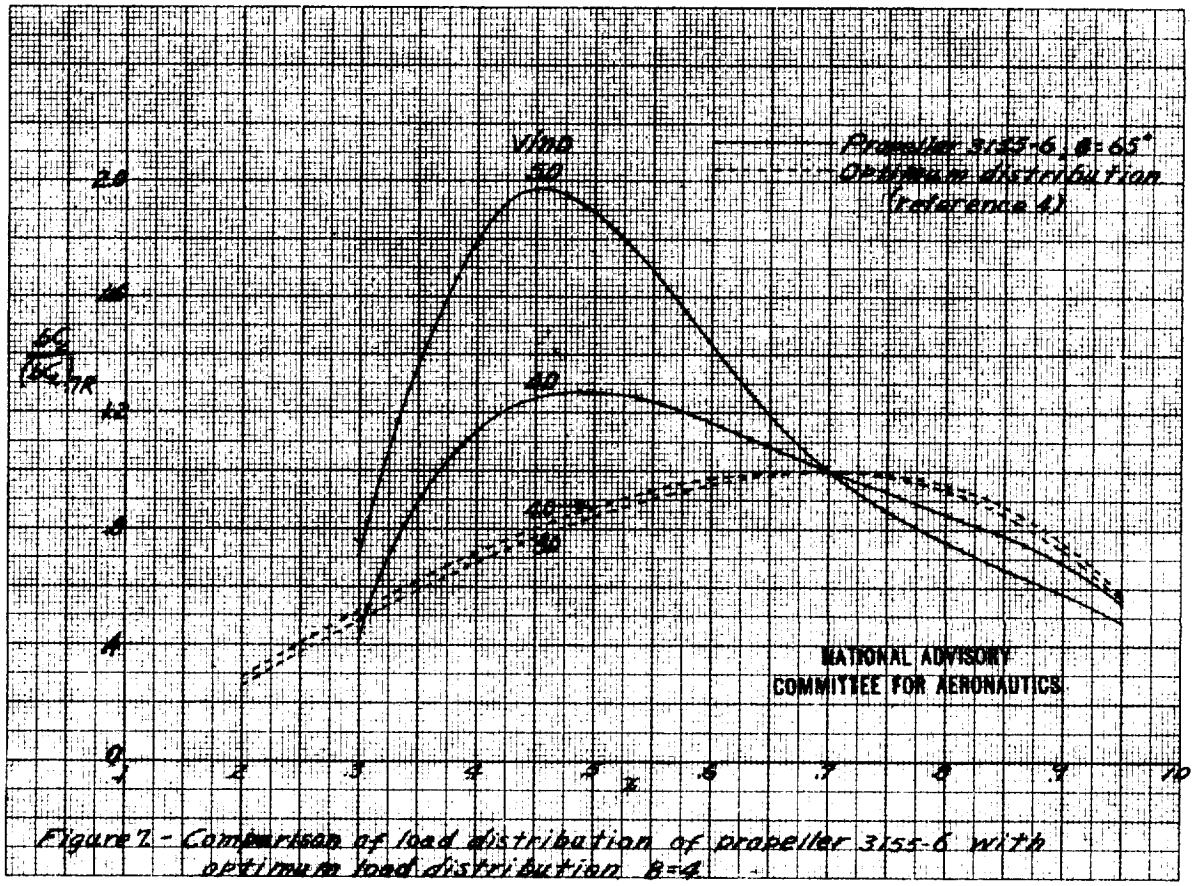

Figure 7 - Comparison of load distribution of propeller 3155-6 with optimum load distribution B=4

L-362

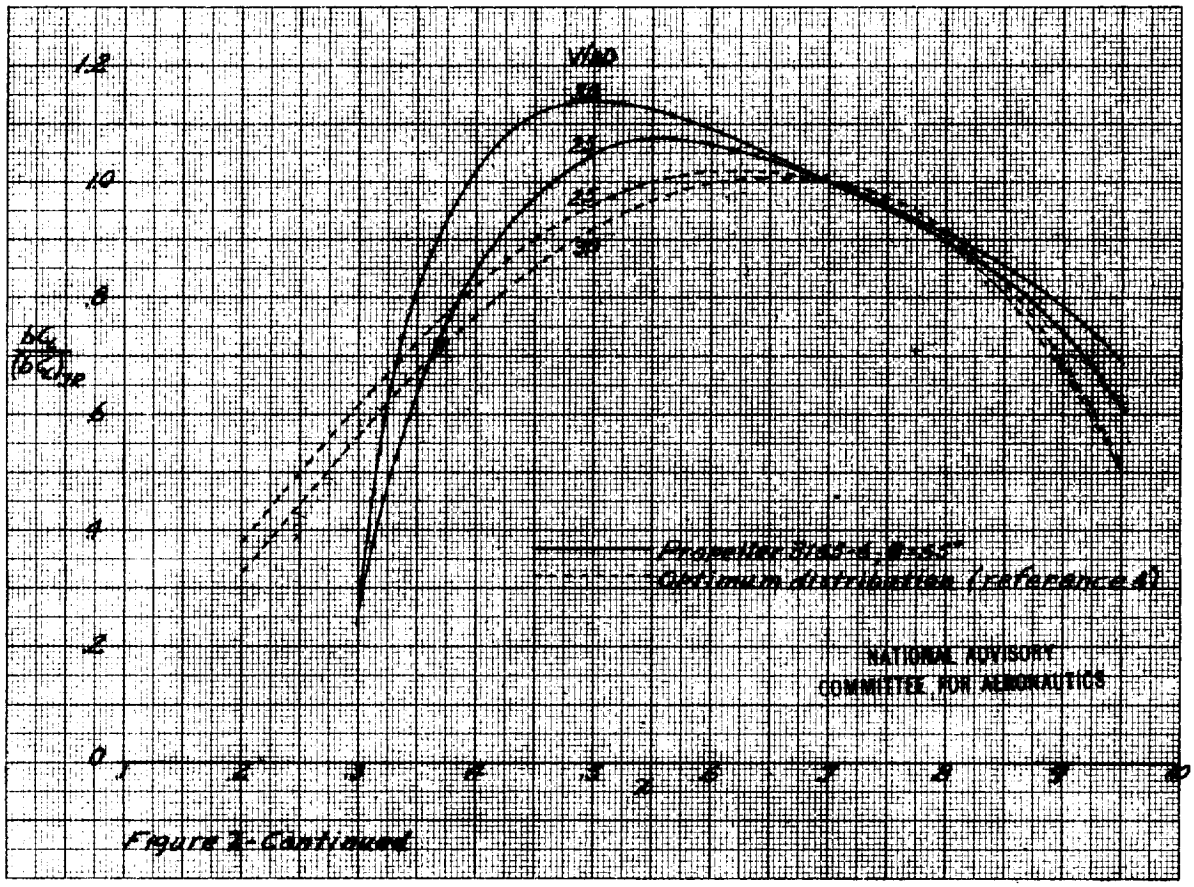

Figure 2.-Continued.

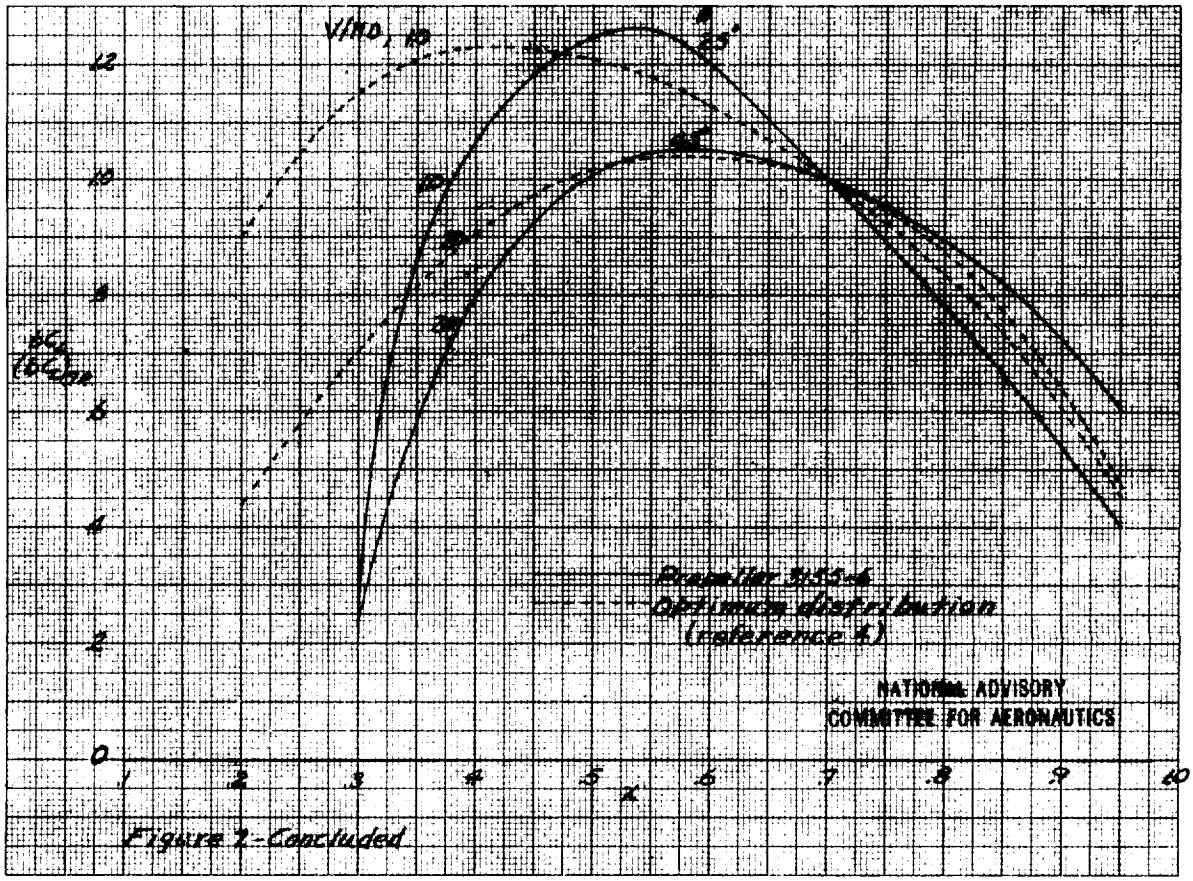

Figure 2.-Concluded.

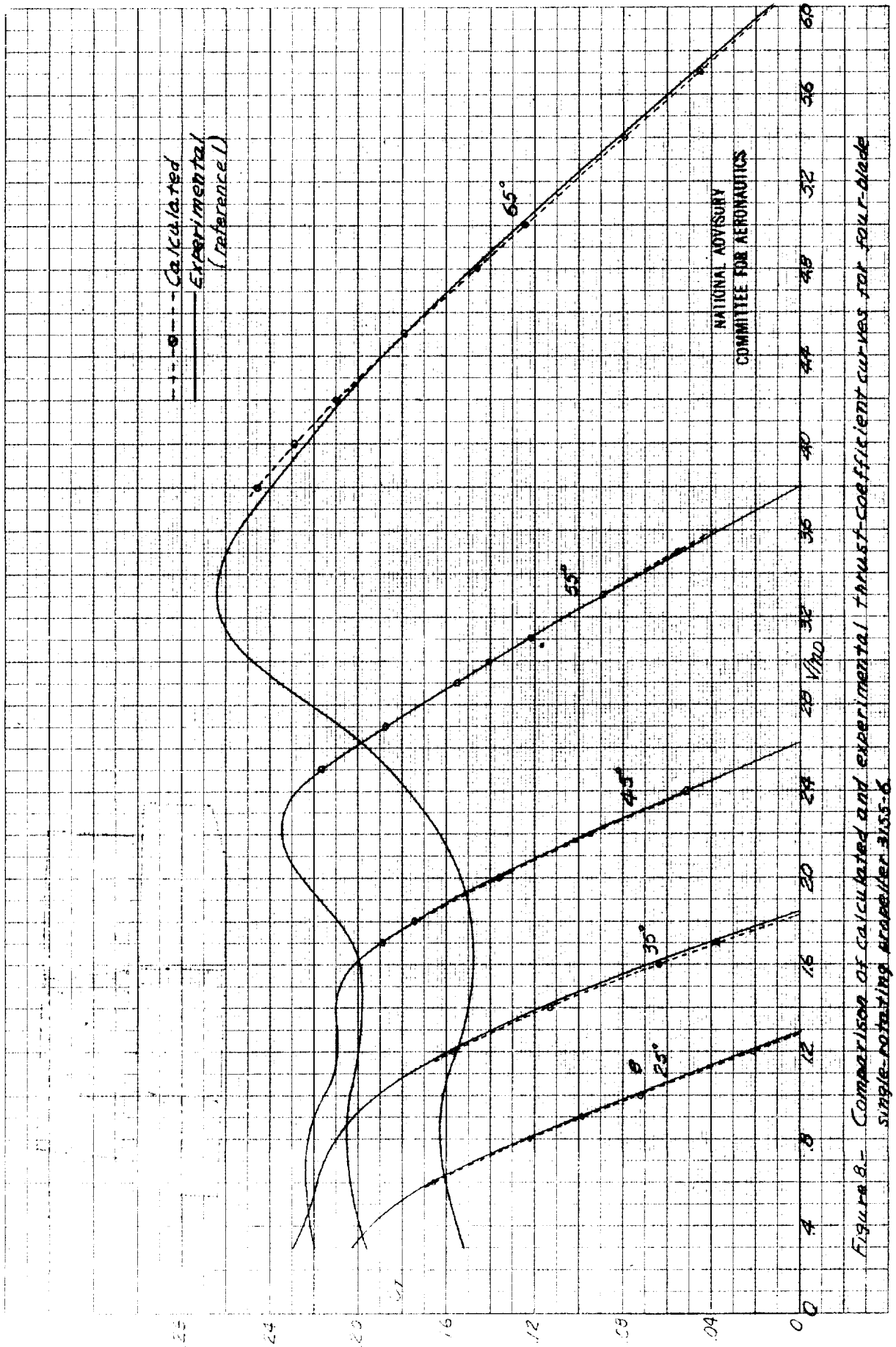

Figure 8.- Comparison of calculated and experimental thrust-coefficient curves for four-blade single-rotating propeller 3155-6.

L-362

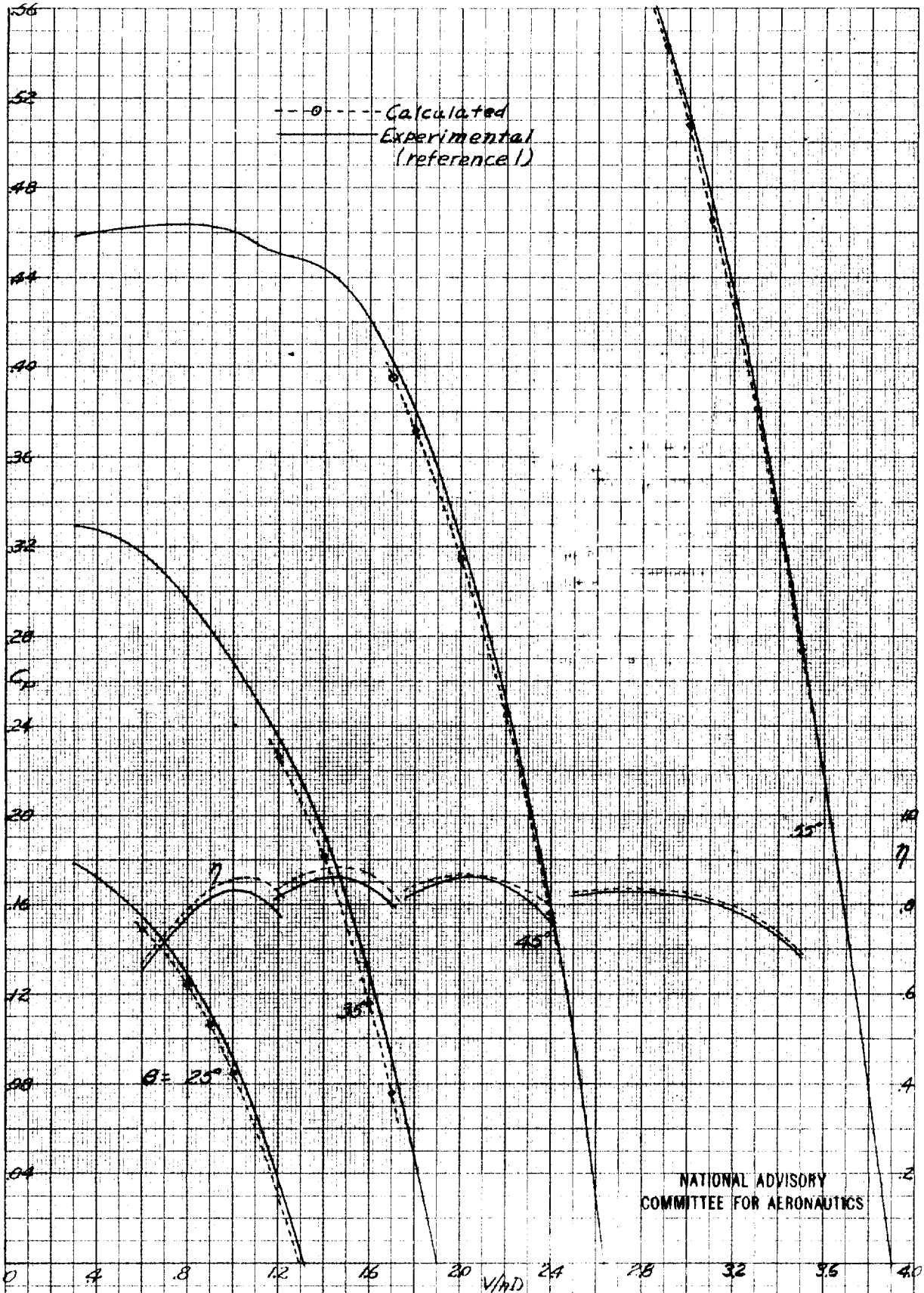

Figure 9.- Comparison of calculated and experimental power-coefficient and efficiency curves for four-blade single-rotating propeller 3655-6

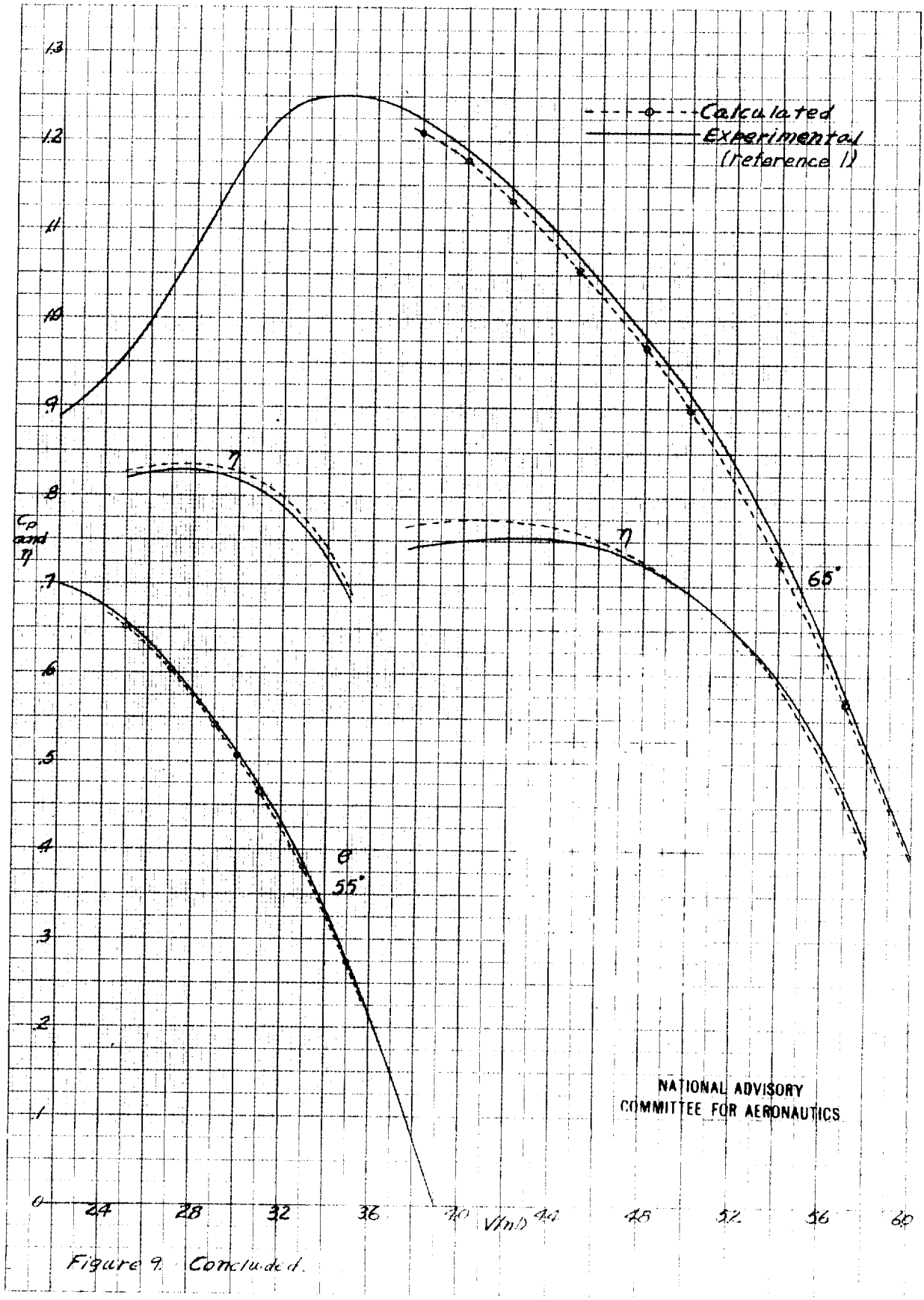

Figure 9. Concluded.

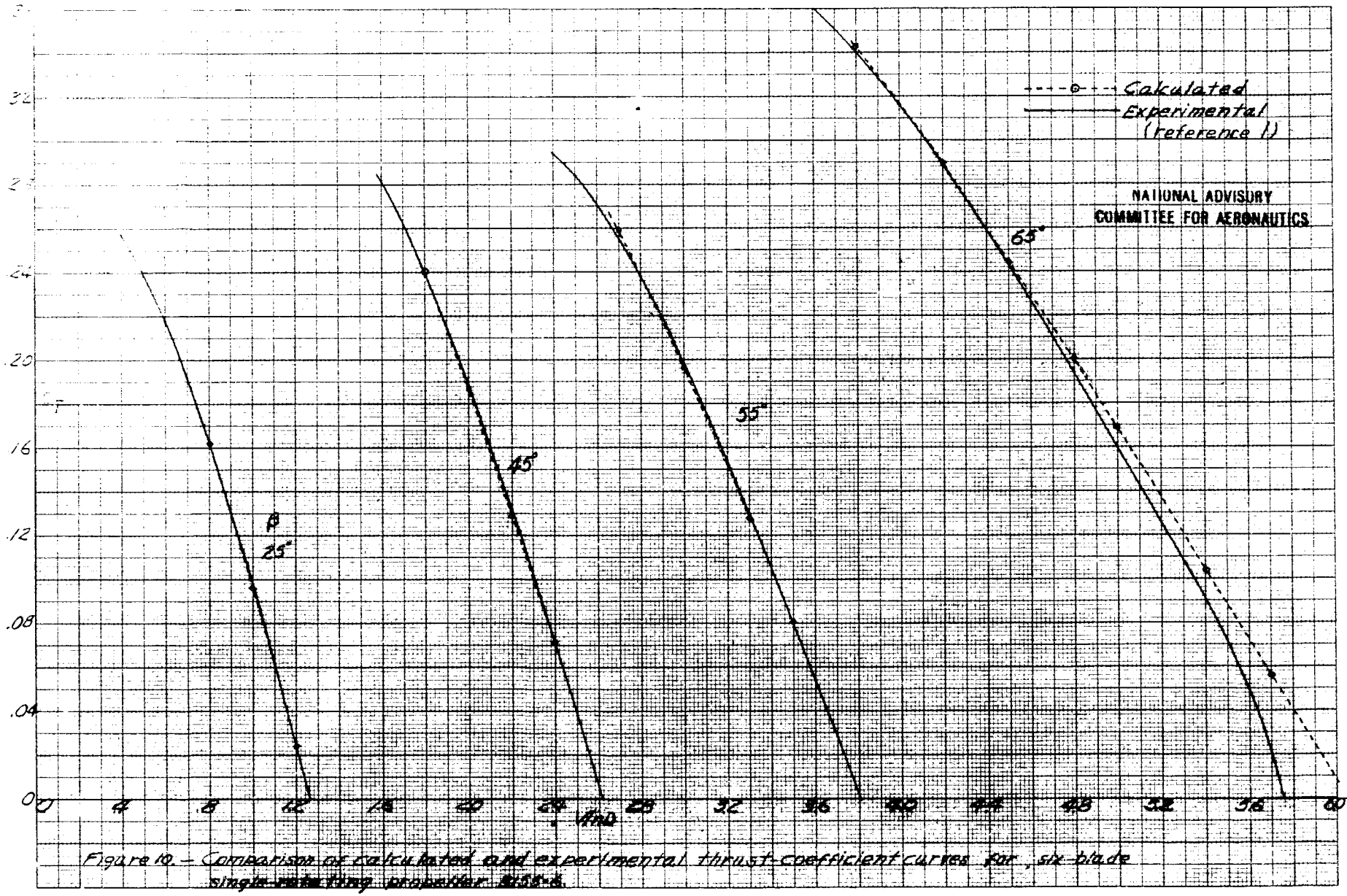

Figure 10. – Comparison of calculated and experimental thrust-coefficient curves for a six-blade single-rotating propeller.

L-362

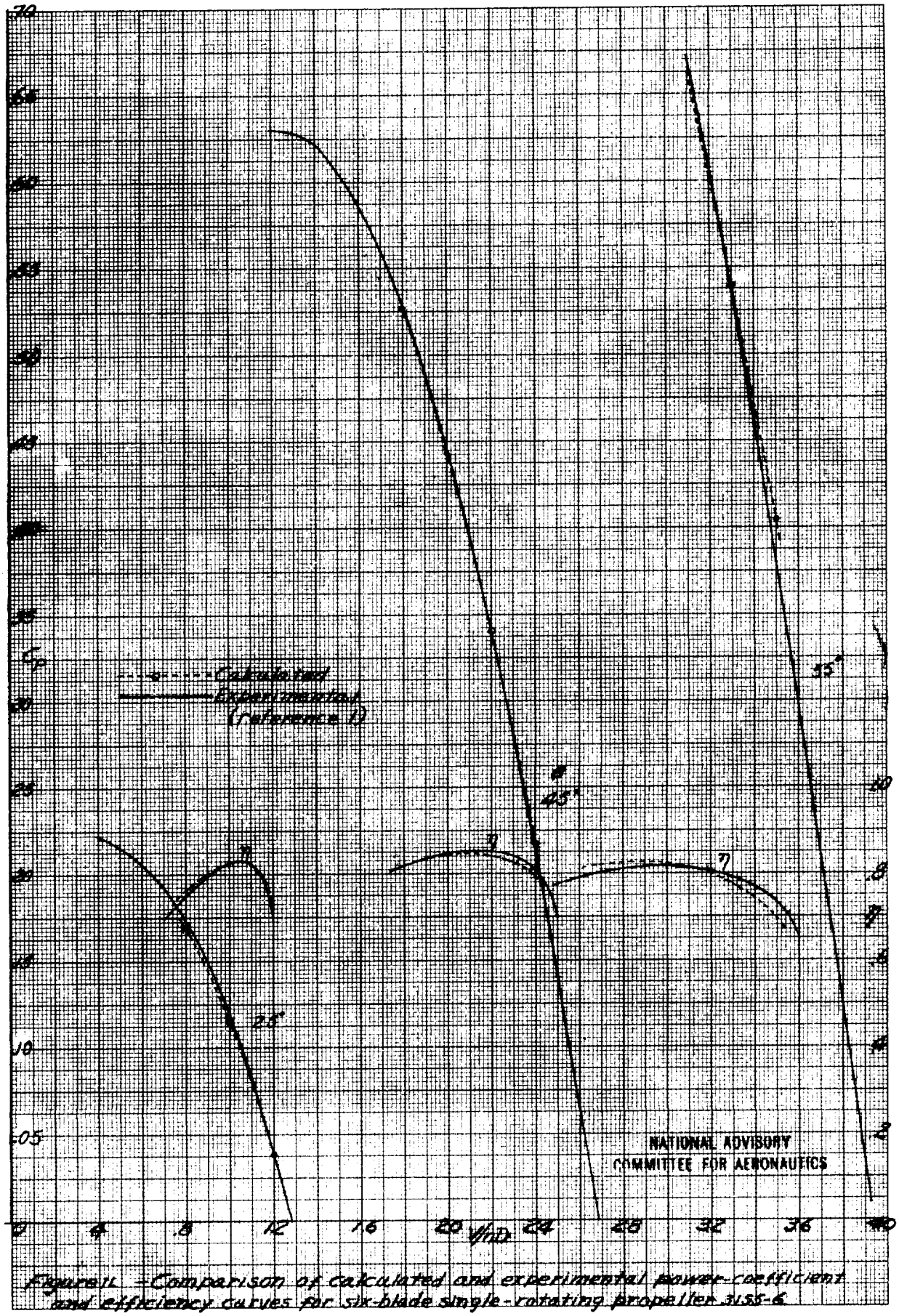

Figure 11.- Comparison of calculated and experimental power-coefficient and efficiency curves for six-blade single-rotating propeller 3155-6.

L-362

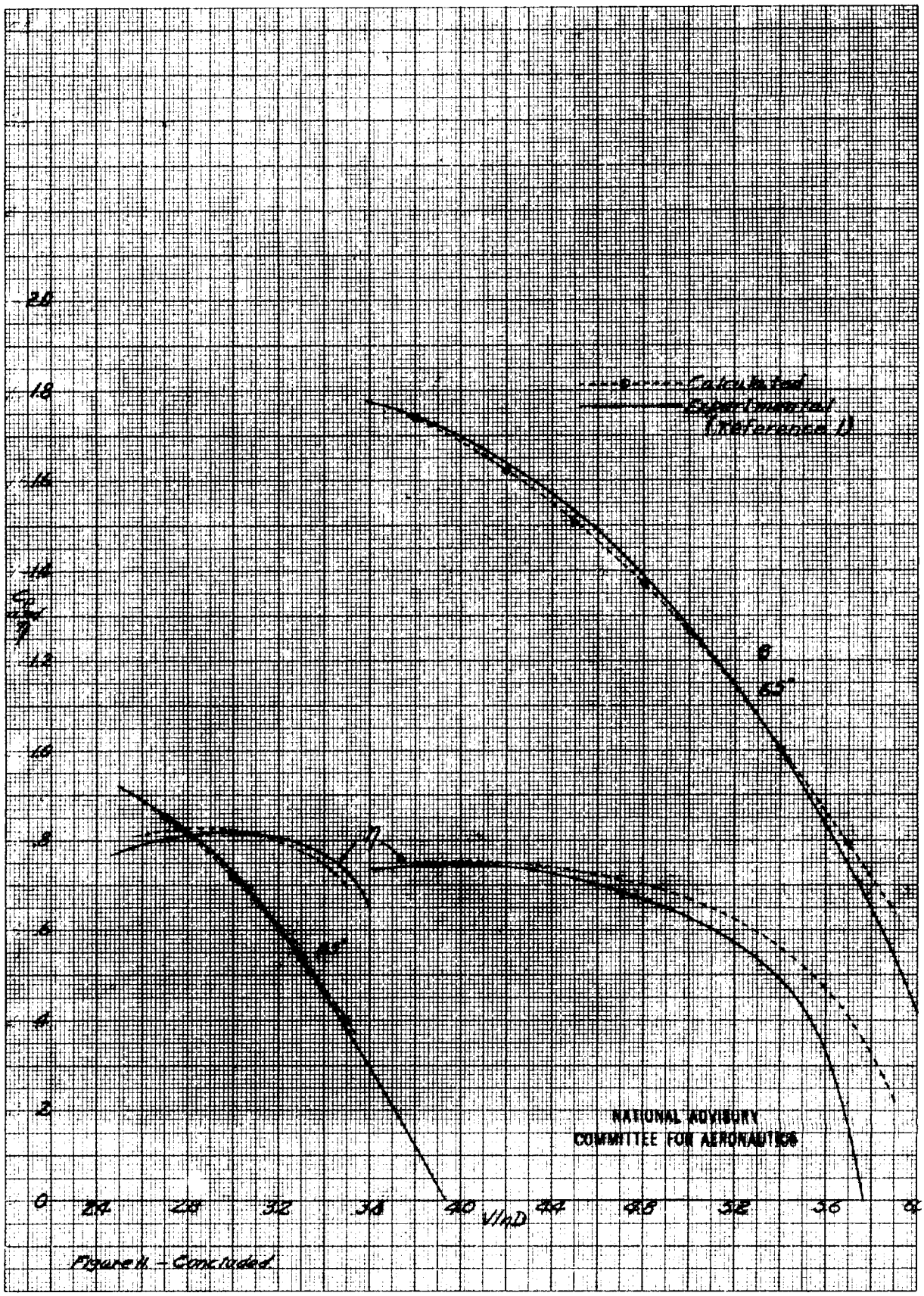

Figure 11. - Concluded

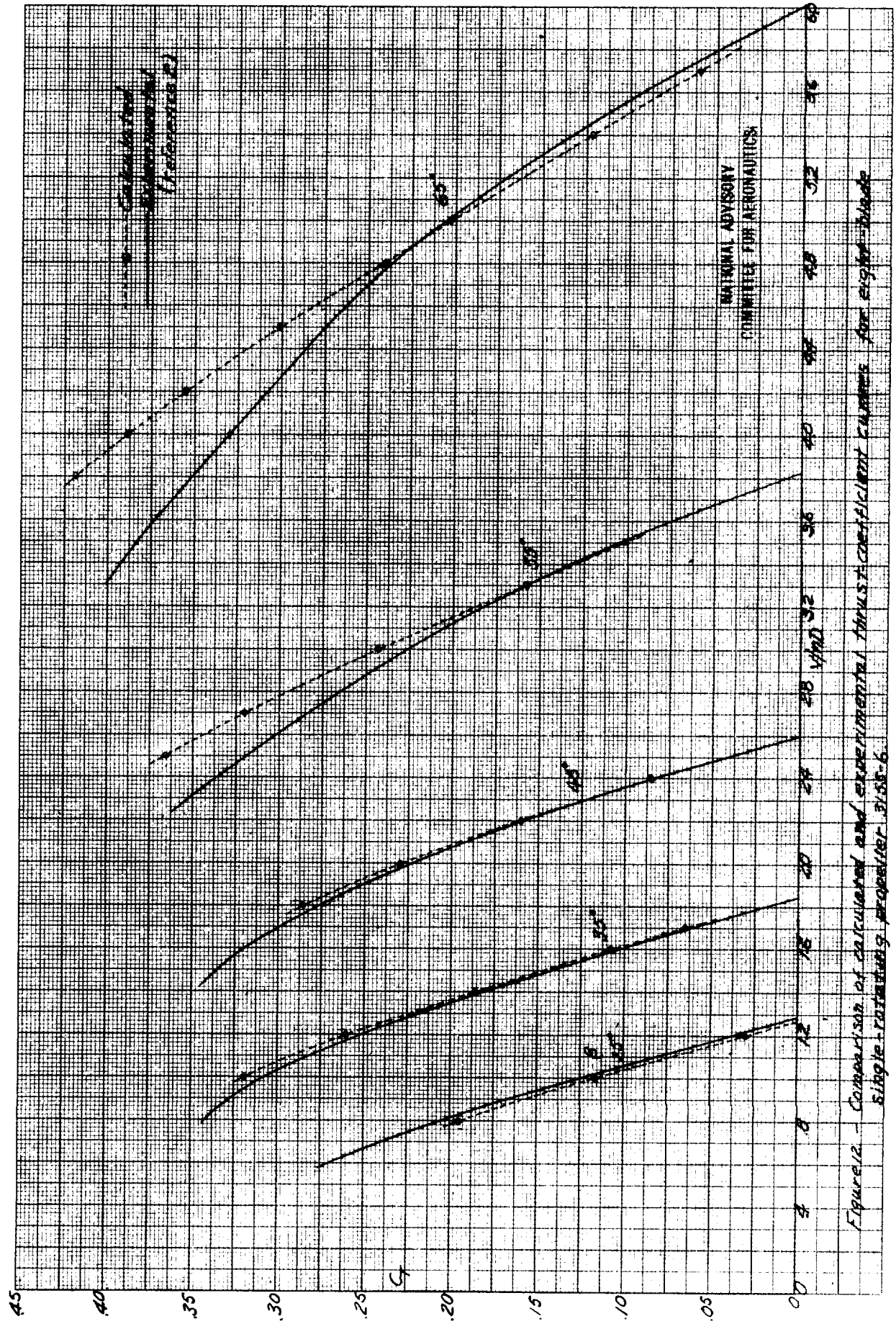

Figure 12 - Comparison of calculated and experimental thrust coefficient curves for eight-blade single-rotating propeller. 3155-6.

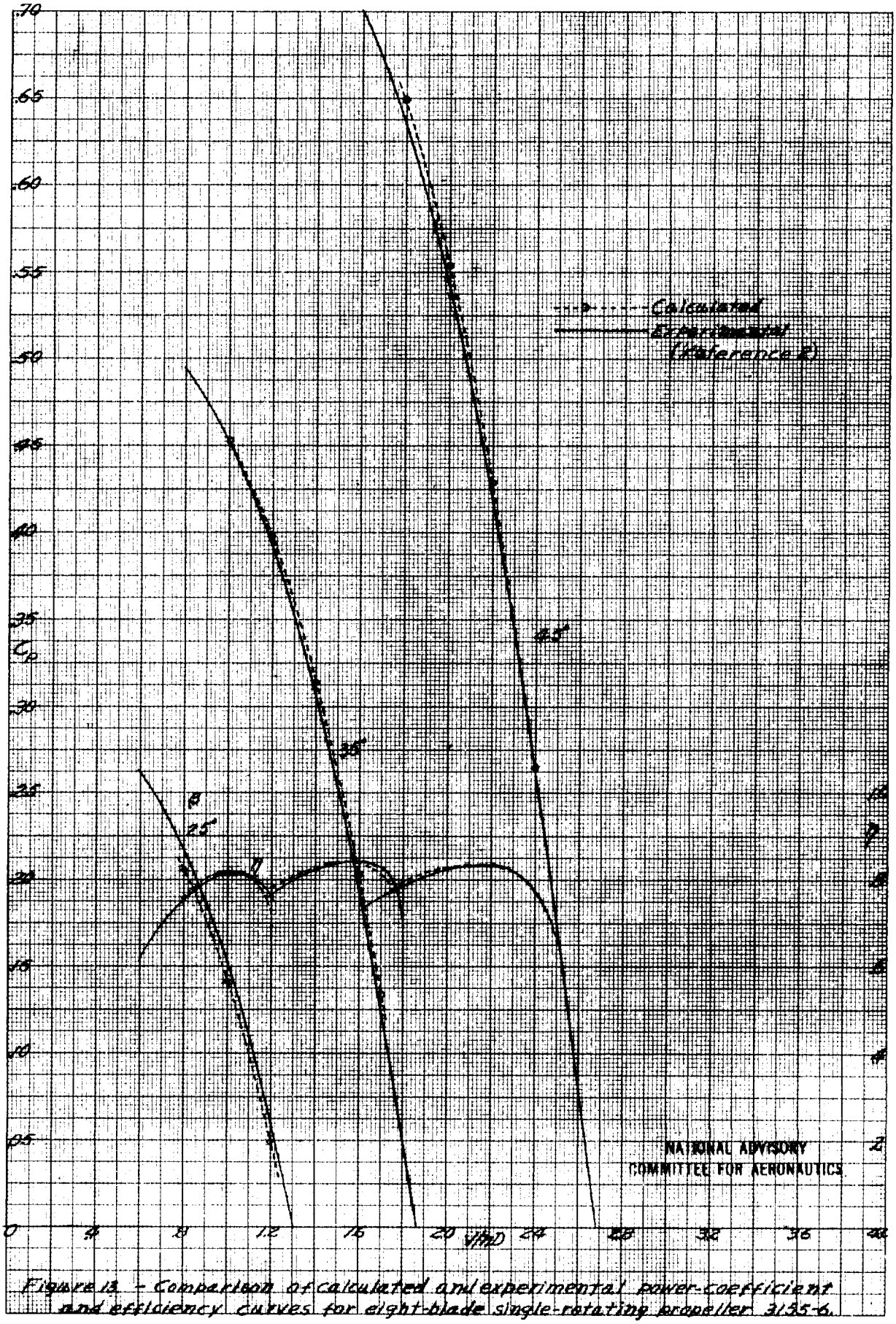

Figure 13. - Comparison of calculated and experimental power-coefficient and efficiency curves for eight-blade single-rotating propeller 3155-6.

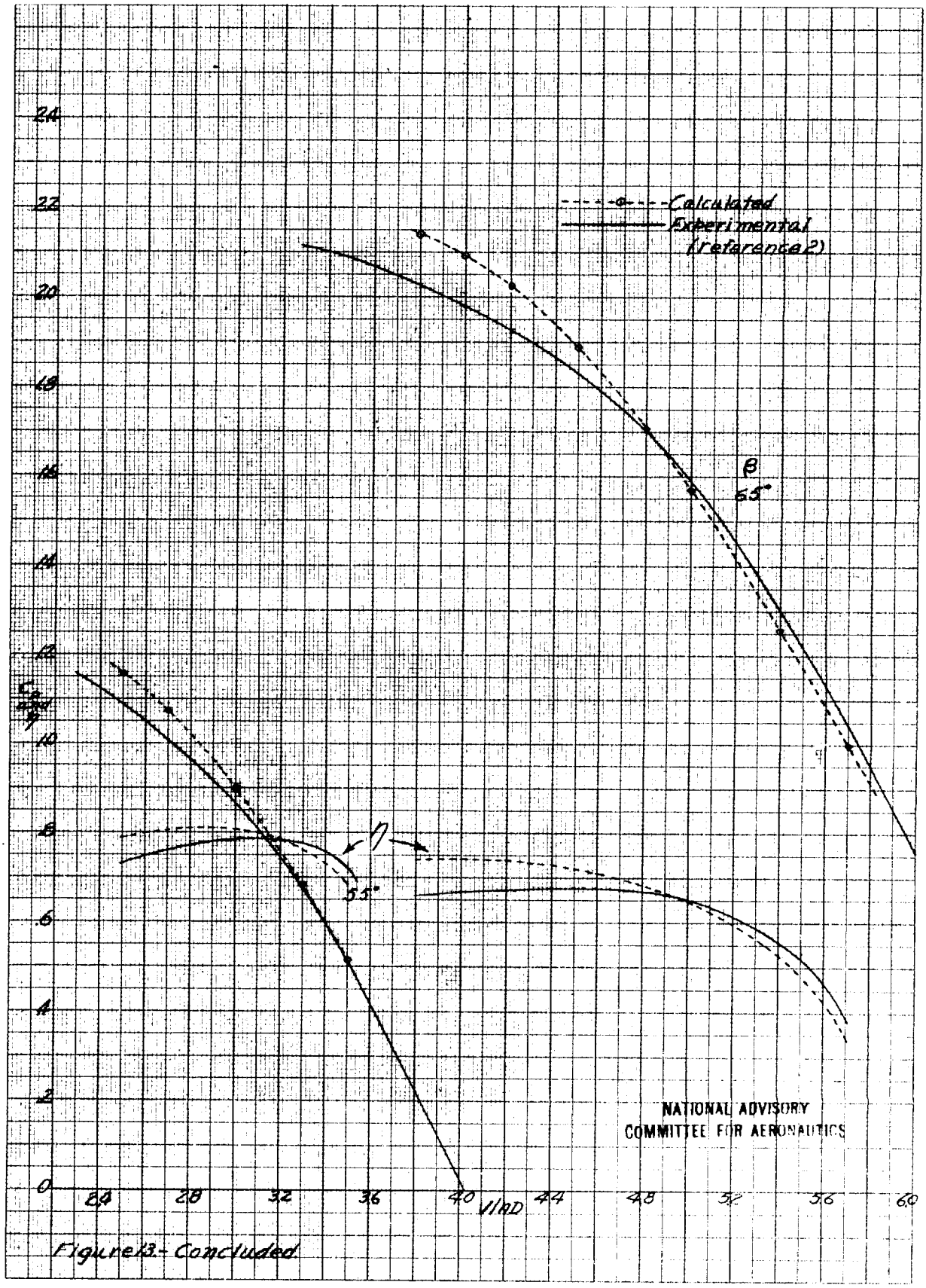

Figure 13.- Concluded.

L-362

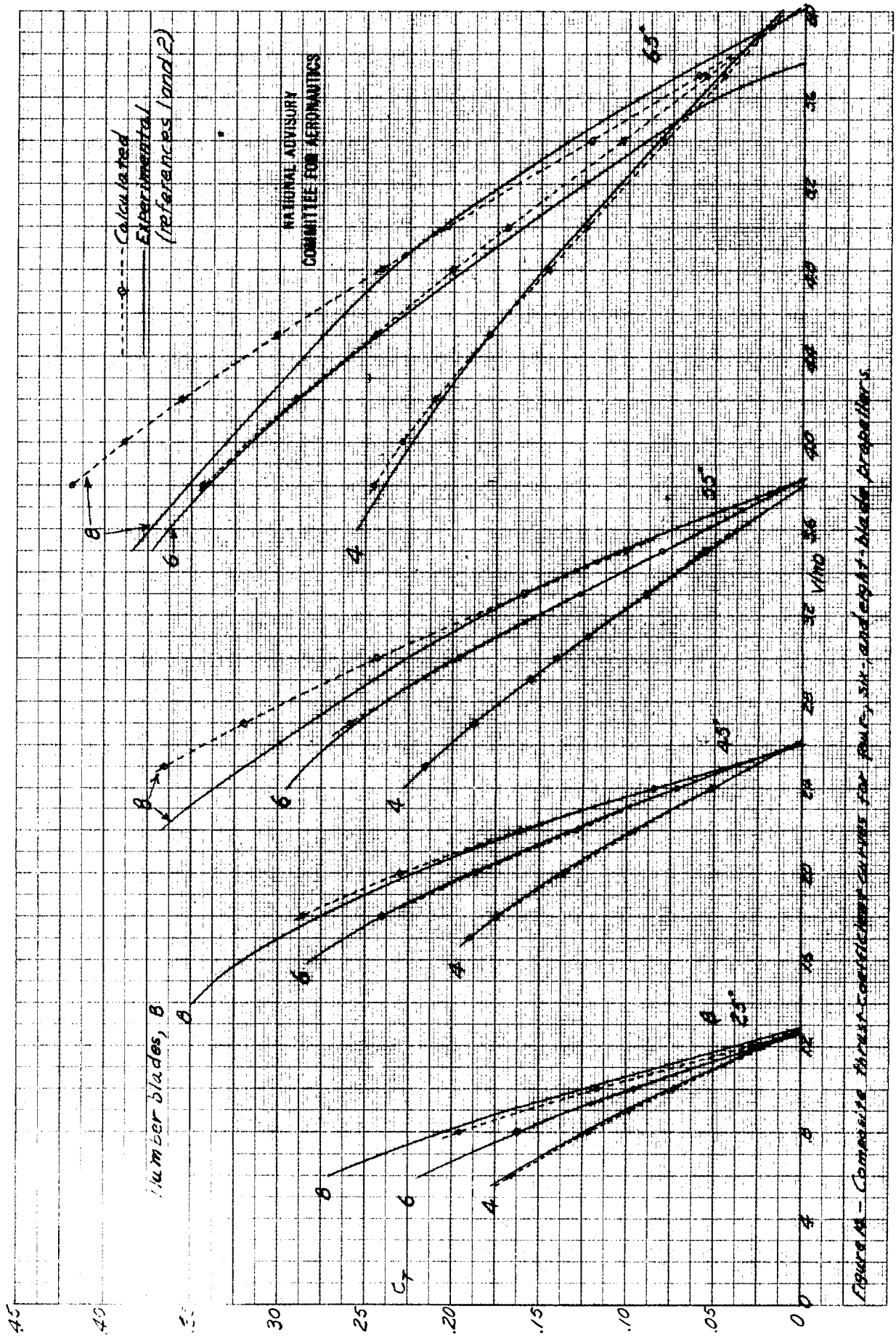

Figure 14.- Composite thrust-coefficient curves for four-, six-, and eight-bladed propellers.

L-362

Figure 15.- Comparison of calculated and experimental efficiencies for four-, six-, and eight-blade propellers.